0013-7227/08/$15.00/0
Printed in U.S.A.

Endocrinology 149(11):5706–5712

doi: 10.1210/en.2008-0717

Regulator of G Protein Signaling-4 Controls Fatty Acid and Glucose Homeostasis

Irena Iankova, Carine Chavey, Cyrielle Clapé, Claude Colomer, Nathalie C. Guérineau, Nicolas Grillet, Jean-François Brunet, Jean-Sébastien Annicotte, and Lluis Fajas

Institut National de la Santé et de la Recherche Médicale, Unité 834 (I.I., C.Ch., C.Cl., J.-S.A., L.F.), Institut de Recherche en Cancérologie de Montpellier (I.I., C.Ch., C.Cl., J.-S.A., L.F.), Institut de Recherche en Cancérologie de Montpellier, Institut National de la Santé et de la Recherche Médicale Unité 896 (I.I., C.Ch., C.Cl., J.-S.A., L.F.), Université Montpellier 1, and Centre Régional de Lutte Contre le Cancer Val d'Aurelle (I.I., C.Ch., C.Cl., J.-S.A., L.F.), Montpellier F-34298, France; Institut National de la Santé et de la Recherche Médicale Unit 661 (C.Co., N.C.G.), Centre National de la Recherche Scientifique UMR5203 (C.Co., N.C.G.); Universités Montpellier 1 and 2 (C.Co., N.C.G.); Institut de Génomique Fonctionnelle (C.Co., N.C.G.), F-34094 Montpellier, France; Centre National de la Recherche Scientifique (N.G., J.-F.B.), Unité Mixté de Recherche 8542, Ecole Normale Supérieure, F-75005 Paris, France; The Scripps Research Institute (N.G.), La Jolla, California 92037; and Centre Hospitalier Universitaire Arnaud de Villeneuve (L.F.), F-34000 Montpellier, France

Circulating free fatty acids are a reflection of the balance between lipogenesis and lipolysis that takes place mainly in adipose tissue. We found that mice deficient for regulator of G protein signaling (RGS)-4 have increased circulating catecholamines, and increased free fatty acids. Consequently, RGS4$^{-/-}$ mice have increased concentration of circulating free fatty acids; abnormally accumulate fatty acids in liver, resulting in liver steatosis; and show a higher degree of glucose intolerance and decreased insulin secretion in pancreas. We show in this study that RGS4 controls adipose tissue lipolysis through regulation of the secretion of catecholamines by adrenal glands. RGS4 controls the balance between adipose tissue lipolysis and lipogenesis, secondary to its role in the regulation of catecholamine secretion by adrenal glands. RGS4 therefore could be a good target for the treatment of metabolic diseases. (*Endocrinology* 149: 5706–5712, 2008)

WHITE ADIPOSE TISSUE (WAT) homeostasis implicates a complex regulatory network of signaling and transcriptional events resulting in a coordinated response to external stimuli. Under nutritional profusion, hormonal signaling results in increased energy storage in adipose tissue in form of triglycerides. Under nutritional deprivation stored triglycerides (TGs) are hydrolyzed in adipose tissue, providing free fatty acids (FFAs) to other tissues, which act as oxidative substrates to maintain energy requirements. Adipose tissue lipolysis comprises sequential hydrolysis of TGs, resulting in glycerol and nonesterified fatty acids (NEFAs), which are released into circulation as FFAs to be taken up by other tissues. Adipose tissue lipases, such as hormone-sensitive lipase (HSL), or adipose triglyceride lipase, whose activity is hormonally and nutritionally regulated, are the final effectors of TG hydrolysis. In the postprandial state, insulin levels are increased. Insulin signaling through the phosphatidylinositol 3-kinase/Akt pathway results in the phosphorylation and subsequent activation of the phosphodiesterase 3B. Activated phosphodiesterase 3B generates AMP from cAMP, resulting in the depletion of cAMP. This releases protein kinase A from activation and lipolysis is inhibited through reduction in the phosphorylation-mediated activation of HSL and perilipin (1).

The hypothalamus-pituitary-adrenal axis plays a major role in the regulation of fasting-induced lipolysis. During fasting and in response to hypothalamus-derived stimuli, adrenal glands are activated and secrete catecholamines, which are major signaling hormones (2). Catecholamines are the primary activators of fasting-induced lipolysis (1, 3), although postprandial plasma catecholamine concentration may be higher than in the fasting state, indicating increased sympathetic nervous system activity after meals (reviewed in Ref. 4). Upon binding to β-adrenergic receptors, catecholamines increase intracellular cAMP concentration, resulting in the activation of protein kinase A, which phosphorylates and activates HSL. Phosphorylation of HSL results in increased hydrolytic activity and consequently leads to enhanced TG hydrolysis (1). Other lipases, such as adipose triglyceride lipase are also the final effectors of lipolytic signaling in adipocytes (5). Activation of catecholamine release in adrenal glands is mediated by the G protein-coupled receptors (GPCR), such as the acetylcholine (ACh) receptor, which bind a heterotrimeric G protein complex of α-, β-, and γ-subunits. Agonist binding to GPCR promotes G protein activation by catalyzing GDP-GTP exchange on the α-subunit. GTP-bound α-subunit dissociates from $\beta\gamma$-subunits and regulates downstream effectors. Signaling by GPCR is terminated by the intrinsic GTPase activity of the Gα-subunit, which hydrolyzes bound GTP to GDP, resulting in the reassociation of the G protein heterotrimer. Intrinsic GTPase

First Published Online July 17, 2008

Abbreviations: ACh, Acetylcholine; aP2, adipocyte fatty acid binding protein; FFA, free fatty acids; GPCR, G protein-coupled receptor; Gpd1, glycerol-3-phosphate dehydrogenase; HSL, hormone-sensitive lipase; IPGTT, ip glucose tolerance test; NEFA, nonesterified fatty acids; PEPCK, phosphoenolpyruvate carboxykinase; RGS, regulator of G protein signaling; TG, triglycerides; WAT, white adipose tissue.

***Endocrinology* is published monthly by The Endocrine Society (http://www.endo-society.org), the foremost professional society serving the endocrine community.**

activity is, however, insufficient to inactivate G protein signaling, but the presence of GTPase-activating proteins, such as regulator of G protein signaling (RGS), accelerates GTPase activity, limiting the duration of G protein activation (6). RGS proteins are therefore negative regulators of G protein signaling.

RGS4 is a member of the large family of RGS proteins that defines the R4 class of the family, which differentiates from other classes by having the RGS domain simply flanked by N- and C-terminal sequences with no specific function other than membrane attachment, and GPCR specificity (reviewed in Refs. 7 and 8). RGS4 has been suggested to participate in several physiological processes, such as heart hypertrophy in response to hypertension (9), modulation of neurotransmitter receptors in brain (9), calcium signaling in heart and pancreas (10), neuronal differentiation (9), or schizophrenia (11). The phenotype of $RGS4^{-/-}$ mice could not demonstrate, however, the participation of RGS4 in these processes. Instead, $RGS4^{-/-}$ mice had normal neural development and were viable and fertile. Only small sensory motor deficits, differences in weight, and central integration of painful stimuli were observed in $RGS4^{-/-}$ compared with $RGS4^{+/+}$ mice (9). Compensation by other RGS family members, or genetic background specificity could mask the analysis of the participation of RGS4 in physiology.

The differences in weight observed in $RGS4^{-/-}$ mice prompted us to investigate the participation of this protein in metabolic processes. We show now that RGS4 controls adipose tissue lipolysis through regulation of the secretion of catecholamines by adrenal glands in response to fasting. $RGS4^{-/-}$ mice have increased concentration of serum catecholamines, increased circulating FFAs, accumulation of fatty acids in liver, resulting in liver steatosis, and show a higher degree of glucose intolerance, when mice are fed with high-fat diet.

Materials and Methods

Animals

Generation of $RGS4^{-/-}$ mouse line has been previously described (9). Only male mice were used. Animals were maintained in a temperature-controlled (23 C) facility with a 12-h light, 12-h dark cycle and had access to food and water *ad libitum* unless indicated otherwise. The control and high-fat diet were obtained from UAR (Villemoisson-sur-Orge, France). This study was conducted according to the local animal ethics board of Institut de Recherche en Cancérologie de Montpellier. The number of animals used was n = 5–8 for wild-type ($RGS4^{+/+}$) and RGS4 knockout ($RGS4^{-/-}$) mice as indicated.

Materials

All chemicals, except if stated otherwise, were purchased from Sigma (St. Louis, MO).

RNA isolation, reverse transcription, and quantitative real-time PCR

RNA was extracted with the use of TRI-reagent (Euromedex, Mundolsheim, France) according to the manufacturer's recommendations. Reverse transcription of total RNA was performed at 37 C using the Muloney murine leukemia virus reverse transcriptase (Invitrogen SARL, Pergy-Pointoise, France) and random hexanucleotide primers (Promega, Madison, WI), followed by a 15-min inactivation at 70 C. Quantitative PCR was carried out by real-time PCR using a LightCycler and SYBR Green light cycler master mix (Roche Applied Science, Mannheim, Germany). Results were normalized to rS9 levels. The primers used were as follows: rS9, 5′-CGGCCCGGGAGCTGTTGACG-3′, 5′-CTGCTTGCGGACCCTAATGTGACG-3′; adipocyte fatty acid binding protein (aP2), 5′-AACACCGAGATTTCCTTCAA-3′, 5′-AGTCACGCCTTTCATAACACA-3′; glycerol-3-phosphate dehydrogenase (Gpd1), 5′-CGTTGGGGCTGGCTTCTGTGAT-3′, 5′-GCCCCTGTAGCTTCTGCCCATTTA-3′; phosphoenolpyruvate carboxykinase (PEPCK), 5′-GGCCCCGGGAGTCACCATCA-3′, 5′-TGCCGAAGTTGTAGCCGAAGAAGG-3′; RGS4, 5′-GAAGAAGATTTTCAACCTGATGG-3′, 5′-GAACTCTTGGCTCCTTTCTGC-3′.

Cell culture, retroviral infection, and Oil Red O staining of 3T3L1 cells

3T3-L1 and 293 cells were grown in DMEM supplemented with 10% fetal bovine serum, 100 U/ml penicillin, and 100 μg/ml streptomycin. 3T3-L1 cells were differentiated with DMEM, 10% serum, 0.5 mM 3-isobutyl-1-methylxanthine, 10 μg/ml insulin, 1 μM dexamethasone, and 1 μM rosiglitazone for 2 d. From d 3 on, cells were incubated with DMEM, 10% serum, 10 μg/ml insulin, and 1 μM rosiglitazone. Oil Red O staining was performed as described (12). Briefly, 3T3-L1 cells were grown on coverslips, fixed in 4% formaldehyde in PBS for 15 min at 4 C, and stained with Oil Red O for 20 min at room temperature. Stock solution of Oil Red O was prepared at 0.5% in isopropanol, and working solution was prepared at 3:2 ratio Oil Red O/deionized water. Cells were rinsed with deionized water and slides were mounted with Mowiol. For retroviral infection, RGS4 cDNA, purchased from Origene (Rockville, MD), was cloned in pBabe Puro vector (cloning details are available on request). Virus production and infection of 3T3-L1 cells was performed as described previously (13). Infection efficiency was estimated at 90%. Pooled clones were differentiated as described.

Protein expression assays

For protein extraction tissues were homogenized with Lysing Matrix D beads (MP Biomedicals Europe, Illkirch, France), using a MagNa Lyser instrument (Roche Applied Science) in a lysis buffer containing 20 mM Tris-HCl (pH 7.4), 137 mM NaCl, 1 mM $MgCl_2$, 1 mM $CaCl_2$, 1 mM dithiothreitol, 10% glycerol, and 0.5% Nonidet P-40. A protease inhibitor cocktail (Sigma) and phosphatase inhibitors (1 mM Na_3VO_4, 50 mM NaF, and 5 mM $Na_4P_2O_7$) were added. Lysates were then centrifuged and the supernatant was recovered. Protein concentrations were determined by Bradford method (Bio-Rad, Hercules, CA). SDS-PAGE and electrotransfer was performed as follows. The membranes were blocked 1 h in blocking buffer (PBS, 0,1%Tween 20, 5% skimmed milk). Filters were first incubated overnight at 4 C with pSer563 HSL antibody (Cell Signaling Technology, Danvers, MA) or total HSL antibody (Santa Cruz Biotechnology, Santa Cruz, CA) and then for 1 h at room temperature with a peroxidase conjugate secondary antibody. The complex was visualized with enhanced chemiluminescence (Interchim, Montluçon, France).

Glucose, insulin, FFA, and catecholamine measurements

For the glucose tolerance tests, mice were fasted overnight (18–20 h) and then injected ip with 2 g/kg (dose per kilogram body weight) glucose. For the FFA measurement after insulin injection, mice were injected ip with 0.75 IU/kg after an overnight fast. Blood glucose levels were measured using an Accu Chek Go glucometer (Roche Diagnostics, Mannheim, Germany), FFAs with a NEFA C kit (Wako Chemicals, Neuss, Germany), and serum insulin levels using a mouse ultrasensitive insulin ELISA kit (Mercodia, Uppsala, Sweden). Catecholamines (norepinephrine and epinephrine) were measured in serum collected from mice, and in a secretion medium from acute adrenal slices using a 2-CAT kit (Labor Diagnostica Nord, Nordhorn, Germany).

Lipolysis in vivo

For isoproterenol treatment, mice were fasted for 7 h and injected ip with isoproterenol (10 mg/kg body weight). Blood was collected from the tail before and 15 min after injection. For insulin treatment, mice were fasted overnight (18 h) and injected ip with insulin (0.75 IU/kg body weight). Blood was collected from the tail before and 60 min after

injection. Serum was frozen at −20 C. Serum FFAs were determined with NEFA C kit (Wako Chemicals).

Adrenal medulla studies

Catecholamine release was measured from adrenal slices. Mice were killed by cervical dislocation. Acute slices were prepared as reported previously (14). Briefly, after removal, the glands were kept in ice-cold saline for 2 min and embedded in a 5% agarose solution (agarose, type IX-A; Sigma). The hardened agar block was then glued with cyanoacrylate onto the stage of a vibratome (DTK-1000, D.S.K.; Dosaka EM Co. Ltd., Kyoto, Japan). Slices of 150 μm thickness were then cut with a razor blade and transferred to a storage chamber maintained at 37 C, containing Ringer's saline (in millimoles): 125 NaCl, 2.5 KCl, 2 $CaCl_2$, 1 $MgCl_2$, 1.25 NaH_2PO_4, 26 $NaHCO_3$, and 12 glucose and buffered to pH 7.4. The saline was continuously bubbled with carbogen (95% O_2-5% $C0_2$). All the slices cutting from a single adrenal were pooled in the same incubation well. Slices were kept for 15 min at 37 C, and then fresh medium was added and a control prestimulation sample was collected. Acetylcholine at 100 μM was then added, and aliquots were collected at different time points and stored at −20 C. Catecholamines (norepinephrine and epinephrine) were measured in the secretion medium using a 2-CAT kit (Labor Diagnostica Nord). Data were expressed as a ratio per protein and total catecholamine content.

Pancreatic islet studies

Islet isolation and insulin secretion studies were described previously (15). Pancreas was digested by collagenase (3 mg/ml) and isolated in oxygenated Krebs-Ringer buffer (in millimoles): NaCl 120; KH_2PO_4 4; $MgSO_4.7H_2O$ 1; $CaCl_2.2H_2O$ 0.75; $NaHCO_3$ 10; HEPES 30 (pH 7.4). Islets were equilibrated for 1 h in presence of 10 mM glucose. Approximately five islets per condition were handpicked and exposed to either 2.8 or 20 mM glucose, in presence or absence of 1 or 10 μM carbachol. Medium containing the released insulin was collected 1 h later. Total insulin of islets was extracted using acid ethanol (75% EtOH, 0.2 M HCl) and measured using a mouse ultrasensitive insulin ELISA kit (Mercodia). Total islet protein concentration was determined using Bio-Rad protein assay (Bio-Rad). Data were expressed as a ratio per protein and total insulin content.

Oil Red O staining of liver

Livers from $RGS4^{+/+}$ and $RGS4^{-/-}$ mice were frozen in O.C.T. Embedding Matrix, (Cell Path, Newtown, UK), sectioned, postfixed in 4% formaldehyde for 10 min at room temperature, and stained with Oil Red O. Slides were counterstained with hematoxylin (Vector, Burlingame, CA).

The β-galactosidase (lacZ) expression assay

Mouse adrenals were collected from $RGS4^{-/-}$ mice and embedded in O.C.T. Embedding Matrix. Tissue blocks were sectioned at 10 μm thickness; postfixed for 20 min in 2% paraformaldehyde and 0.2% glutaraldehyde; washed in PBS (2 × 5 min); and incubated overnight at 37 C in freshly prepared X-gal staining buffer, containing 1 mg/ml X-gal (Euromedex, Mundolsheim, France), 5 mM potassium ferricyanide, 5 mM potassium ferrocyanide, and 2 mM $MgCl_2$ in PBS. Tissue sections were rinsed in PBS and counterstained with 0.1% Gurr's Nuclear Fast Red (Gurr's, London, UK) in 5% aluminum sulfate [$Al_2(SO_4)_3/15H_2O$] for 3–5 min. Mounting solution (Dako, Glostrup, Denmark) and coverslips were added to the sections.

Triglyceride content measurement

For determination of hepatic triglyceride content in $RGS^{+/+}$ and $RGS4^{-/-}$ mice, liver tissue (50–100 mg) was homogenized for 4 min in 2 ml isopropanol with a Polytron disrupter. The homogenate was centrifuged at 2000 × *g* for 10 min, and 10 μl of the resulting supernatant were dried with a Speedvac system (Jouan, Saint-Herblain, France). The dry residue was dissolved in 5 μl isopropanol, and its TG content was measured with triglyceride FS kit (Diasys Diagnostic Systems, Holzheim, Germany). For muscle TGs, tissue (100–150 mg) was homogenized with Lysing Matrix D beads (MP Biomedicals Europe), using a MagNa Lyser instrument (Roche Applied Science) in 1 ml isopropanol. The homogenate was centrifuged at 2000 × *g* for 10 min, and 20 μl of the resulting supernatant were dried with a Speedvac system. The dry residue was dissolved in 5 μl isopropanol and then proceeded as for hepatic triglyceride content. All values of tissue triglyceride content were corrected for tissue weight.

Statistical analysis

Data are presented as means ± SEM. Group means were compared by factorial ANOVA. Differences were considered statistically significant at $P < 0.05$.

Results

Increased fasting FFAs in RGS4−/− mice and β-agonist-induced lipolysis in adipose tissue of RGS4−/− mice

Previous studies showed decreased body weight in $RGS4^{-/-}$ compared with $RGS4^{+/+}$ mice, suggesting the implication of RGS4 in adipose tissue biology (9). We therefore first analyzed whole-body and relative WAT weights in these mice. No significant differences were observed in either body or WAT weights (Fig. 1, A and B). In contrast, we found consistent and significantly increased circulating fasting FFA in $RGS4^{-/-}$ compared with $RGS4^{+/+}$ mice, independent of body or WAT weights (Fig. 1C). Because no differences in food intake (data not shown) or WAT weight (Fig. 1B) could be demonstrated, the increase in circulating FFAs observed in $RGS4^{-/-}$ mice suggested impaired WAT metabolism, pointing to abnormal fasting-induced lipolysis. To explore this hypothesis, we analyzed the response of $RGS4^{+/+}$ and $RGS4^{-/-}$ mice to lipolytic stimulation. A 3-fold increase in FFA release, as measured by the concentration of circulating FFA in serum of $RGS4^{+/+}$ mice, was observed in response to the β-adrenergic agonist isoproterenol (Fig. 1D). Interestingly, $RGS4^{-/-}$ mice, which showed increased FFA basal levels were significantly ($P < 0.05$) less responsive to isoproterenol compared with $RGS4^{+/+}$ mice (1.5-fold compared with 3-fold stimulation; Fig. 1D). This suggested that RGS4 is implicated in the response of WAT to lipolytic stimulation. Next, the antilipolytic effects of insulin were tested. Insulin administration to fasted $RGS4^{+/+}$ mice resulted, as expected, in a 2.5-fold decrease in circulating FFA (Fig. 1E). An almost identical decrease in circulating FFA levels was observed when $RGS4^{-/-}$ mice were insulin stimulated (Fig. 1E). These results indicated that the antilipolytic mechanisms are not impaired in $RGS4^{-/-}$ mice. Furthermore, increased lipolysis in WAT of $RGS4^{-/-}$ mice was further demonstrated by increased phosphorylation of the rate-limiting lipolytic enzyme, the HSL (Fig. 1F).

Abnormal fatty liver, hyperinsulinemia, and hyperglycemia in RGS4−/− mice

Increased fasting FFA is a risk factor for fatty liver and insulin resistance. A first interesting observation was the pale appearance of liver from $RGS4^{-/-}$ mice, suggesting increased fat accumulation (Fig. 2A). This was further demonstrated by Oil Red O staining (Fig. 2A) and triglyceride quantification analysis, which showed increased TG content in liver from $RGS4^{-/-}$, compared with $RGS4^{+/+}$ mice (Fig. 2B). These differences were further increased when TG con-

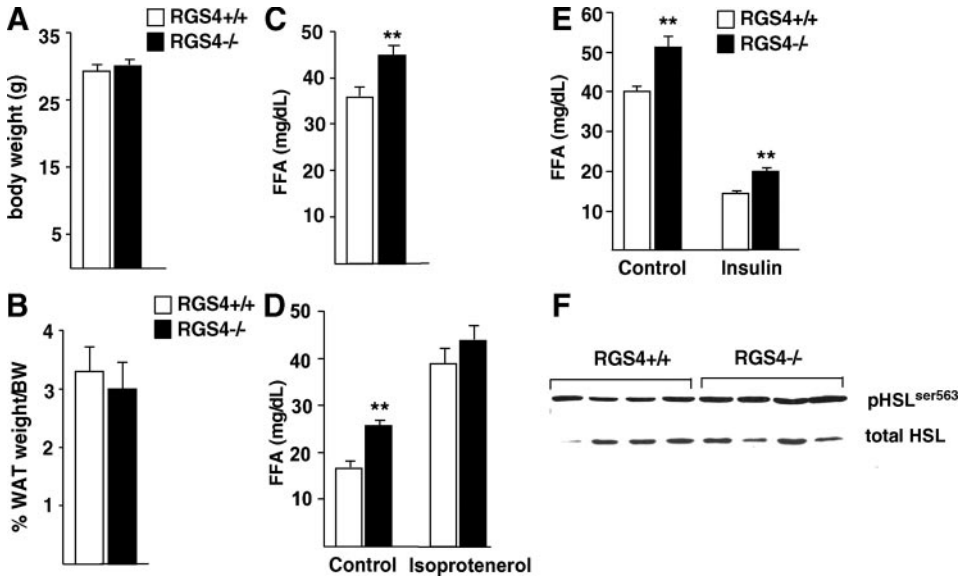

FIG. 1. Adipose tissue weight, fatty acid quantification, and *in vivo* lipolysis analysis in RGS4$^{-/-}$ mice. A, Body weight of RGS4$^{+/+}$ and RGS4$^{-/-}$ mice (RGS4$^{+/+}$, n = 8; RGS4$^{-/-}$, n = 8) was analyzed at 25 wk. B, WAT weight is represented as a percentage of body weight in the same mice. C, Quantification of serum FFA concentration in mice fasted for 16 h. D, Isoproterenol-induced *in vivo* lipolysis in 7 h-fasted RGS4$^{+/+}$ (n = 6) and RGS4$^{-/-}$ (n = 6) mice measured by FFA concentration in serum. Blood serum was collected before (control) and 15 min after injection of isoproterenol (10 mg/kg). E, Analysis of *in vivo* lipolysis in response to insulin in overnight fasted RGS4$^{+/+}$ and RGS4$^{-/-}$ mice. FFA serum levels were determined before (control) and 60 min after ip injection of insulin (0.75 IU/kg). F, Expression of HSL phosphorylated on Ser563 compared with the expression of total HSL was assessed by Western blot. Data are mean ± SEM. Statistically significant differences (ANOVA, $P < 0.05$) are indicated in this and subsequent figures by an *asterisk*.

tent of the livers of high-fat diet-fed RGS4$^{-/-}$ and RGS4$^{+/+}$ mice were analyzed (Fig. 2B). Lipid accumulation in muscles of RGS4$^{-/-}$ compared with RGS4$^{+/+}$ mice was also observed in normal fed mice (Fig. 2C), suggesting a more general effect. Moreover, gene expression analysis showed increased mRNA expression of markers of fatty acid content and synthesis, such as aP2, Gpd1, or PEPCK, in livers of RGS4$^{-/-}$ compared with RGS4$^{+/+}$ mice (Fig. 2D). The increased lipid content in liver was correlated with increased glucose and insulin levels in serum of fasted RGS4$^{-/-}$ mice (Fig. 2, E and F), which was overall consistent with the observed increase in circulating FFAs in RGS4$^{-/-}$ mice.

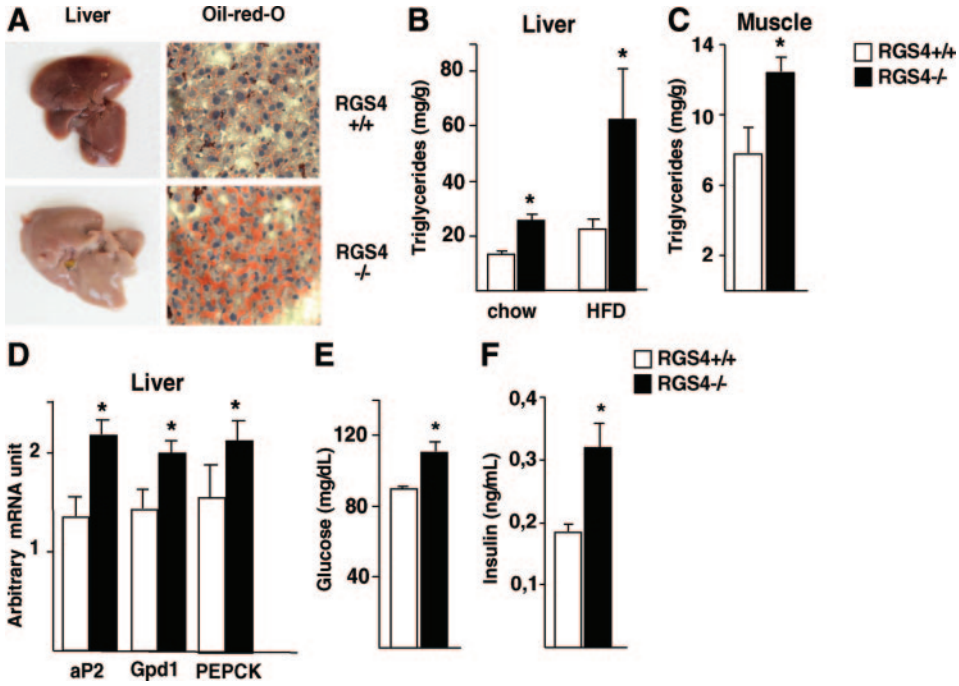

FIG. 2. Lipid content in liver and serum metabolic factors in RGS4$^{-/-}$ mice. A, Representative pictures of whole livers of 25-wk-old RGS4$^{+/+}$ or RGS4$^{-/-}$ mice. *Pale color* is indicative of lipid accumulation. Oil Red O-stained liver sections in the same mice demonstrate lipid content. B, Hepatic TG content in 25-wk-old RGS4$^{+/+}$ (n = 5) and RGS4$^{-/-}$ (n = 5) mice on a chow or high-fat diet for 4 wk. C, Muscle triglyceride content in 25-wk-old RGS4$^{+/+}$ (n = 5) and RGS4$^{-/-}$ (n = 5) normal-fed mice. D, Hepatic expression levels of aP2, Gpd1, and PEPCK in normal-fed mice as determined using quantitative RT-PCR. Serum fasting glucose concentration (E) and insulin serum levels (F) were determined in 18-wk-old RGS4$^{+/+}$ or RGS4$^{-/-}$ mice as indicated.

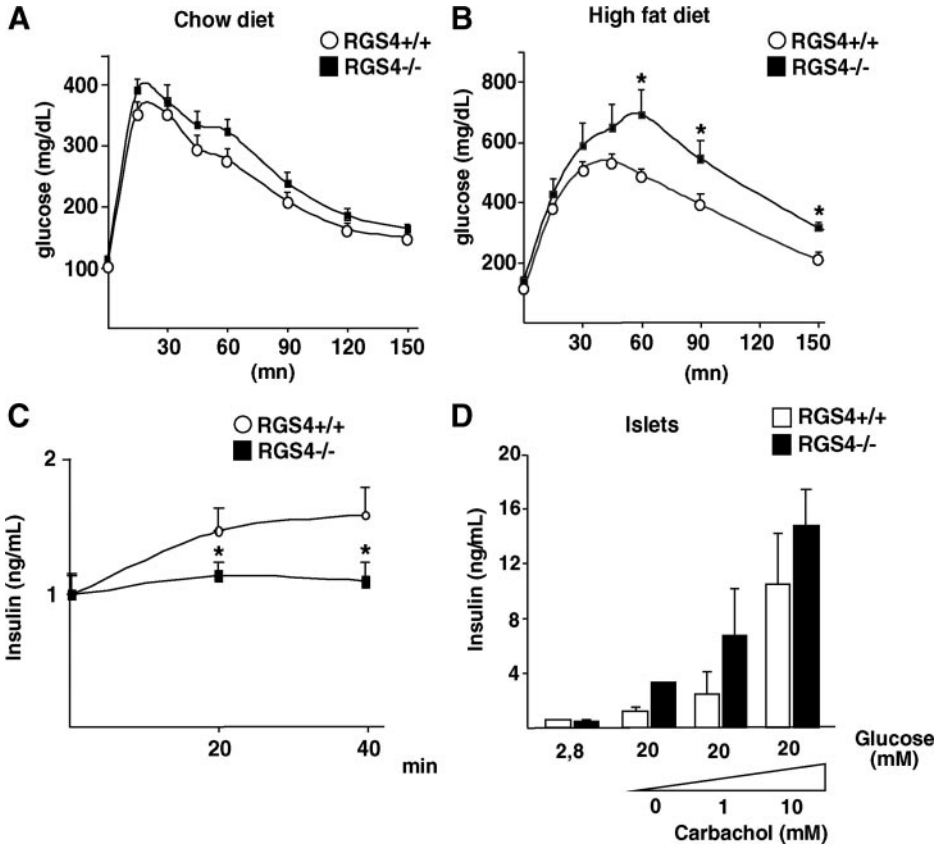

FIG. 3. Glucose homeostasis in RGS4$^{-/-}$ mice. IPGTT in 25-wk-old mice under chow diet (A) (RGS4$^{+/+}$, n = 8; RGS4$^{-/-}$], n = 8) or after 3 wk of high-fat diet (B) (RGS4 $^{+/+}$, n = 5; RGS4 $^{-/-}$, n = 5). Blood glucose concentrations were measured at the indicated time points after ip injection of glucose (2 g/kg). C, Quantification of relative serum insulin levels measured by ELISA test at the indicated time points in the same mice during the IPGTT in A. D, Insulin secretion of isolated islets from RGS4$^{-/-}$ or RGS4$^{+/+}$ mice stimulated for 1 h in the presence of 2.8 or 20 mM glucose and increasing concentrations of carbachol. Results are relative to total insulin and protein content.

Impaired glucose homeostasis and insulin secretion in RGS4$^{-/-}$ mice

Liver steatosis, hyperglycemia, and hyperinsulinemia are strong predictors of insulin resistance. We therefore evaluated glucose homeostasis in RGS4$^{-/-}$ and RGS4$^{+/+}$ mice. Intraperitoneal glucose tolerance test (IPGTT) showed a significant trend of RGS4$^{-/-}$ mice toward glucose intolerance, compared with RGS4$^{+/+}$ mice (Fig. 3A). These differences were even more pronounced when IPGTT was performed on high-fat diet-fed mice (Fig. 3B). Glucose intolerance in RGS4$^{-/-}$ mice was correlated with a decrease in insulin secretion in response to a glucose load (Fig. 3C). These results strongly suggested that RGS4 is implicated in the control of glucose homeostasis.

Decreased insulin secretion could point to either an intrinsic defect of RGS4$^{-/-}$ pancreatic β-cells or a toxic effect, secondary to chronically elevated circulating FFAs, such as observed in RGS4$^{-/-}$ mice. Analysis of isolated islets from RGS4$^{-/-}$ or RGS4$^{+/+}$ mice demonstrated that RGS4$^{-/-}$ β-cells were not defective in insulin secretion in response to glucose, when compared with islets from RGS4$^{+/+}$ mice (Fig. 3D), suggesting that the decrease in insulin secretion in response to glucose observed in RGS4$^{-/-}$ mice (Fig. 3C) was rather secondary to the toxic effects of FFAs.

No effects of RGS4 in adipocyte differentiation and lipid content

To elucidate the implication of RGS4 in WAT development or function, we first analyzed RGS4 mRNA expression during the adipocyte differentiation program of 3T3-L1 preadipocytes. RGS4 was expressed in 3T3-L1 preadipocytes, whereas its expression declined during the differentiation process, reaching the limits of detection in fully differentiated adipocytes (Fig. 4A). In addition, no differences in the differentiation capacity was observed, as assessed by Oil Red O staining between 3T3-L1 cells infected with retrovirus expressing either RGS4 or empty vectors (Fig. 4B). Furthermore, the lack of differences in lipid content suggested a normal balance between lipolysis and lipogenesis in RGS4-overexpressing cells. RGS4 overexpression in these 3T3-L1 cells was verified by quantitative PCR (Fig. 4C). Taken together, these results suggested that the observed effects of RGS4 on lipolysis (Fig. 1) were not cell autonomous of WAT.

Increased catecholamine release in RGS4$^{-/-}$ mice

Insulin resistance observed in RGS4$^{-/-}$ mice was likely the result of impaired FFA secretion in WAT. Expression of RGS4 was, however, very low in adipose tissue of mice (Fig. 5A), precluding any effect of this protein in this tissue. Therefore the observed effects of RGS4 might be mediated by hormonal signaling, such as catecholamines, which are key hormones for the regulation of lipolysis. RGS4 was preferentially expressed in the mouse adrenal medulla as well as in the zona glomerulosa as demonstrated using β-gal staining of mouse adrenal and kidney sections (Fig. 5B). Consistent with our hypothesis, serum concentration of both epinephrine and norepinephrine were robustly increased in RGS4$^{-/-}$ compared with RGS4$^{+/+}$ overnight-fasted mice

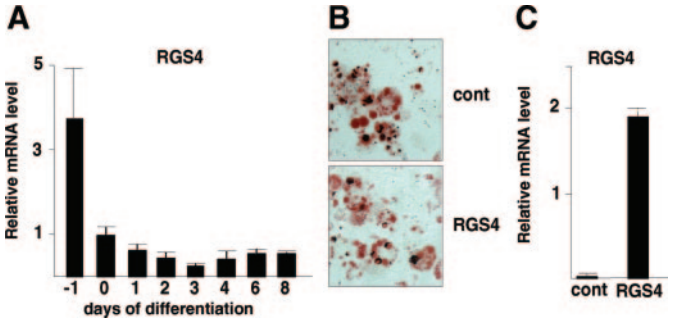

FIG. 4. *RGS4* expression during adipocyte differentiation. A, *RGS4* expression in 3T3-L1 preadipocyte differentiation was determined using quantitative RT-PCR. Results were normalized by the expression level of rS9. B, Oil Red O staining of 3T3-L1 adipocytes expressing either an empty vector (control) or a vector encoding RGS4 8 d after induction of differentiation. C, *RGS4* mRNA expression, analyzed by RT-PCR, in 3T3-L1 empty vector or RGS4 vector-expressing cells.

(Fig. 5C). Interestingly, this increase was abrogated when mice were refed for 4 h (Fig. 5C). This was consistent with the observed increase in basal lipolysis and fasting FFAs in $RGS4^{-/-}$ mice. To elucidate whether this increase in circulating catecholamine levels originated from adrenal glands, the main tissue involved in catecholamine release at the periphery, secretion experiments using acute adrenal slices were performed. Upon ACh stimulation, epinephrine and norepinephrine secretion was up-regulated in glands from $RGS4^{+/+}$ mice, as expected (Fig. 5, D and E). Most interestingly was the observation that adrenal glands from $RGS4^{-/-}$ mice secreted at least 4-fold more epinephrine and norepinephrine in response to ACh stimulation than adrenals from $RGS4^{+/+}$ mice (Fig. 5, D and E). Furthermore, basal catecholamine secretion levels were increased in adrenals from $RGS4^{-/-}$ compared with $^{+/+}$ mice (Fig. 5, D and E). Altogether, these results suggest that RGS4 negatively regulates catecholamine secretion in adrenal glands.

Discussion

Circulating catecholamines are mainly secreted by adrenal glands in response to synaptically released ACh at the splanchnic nerve terminals synapsing onto chromaffin cells. ACh exerts its effects through activation of postsynaptic nicotinic and muscarinic cholinergic receptors (16, 17). RGS4 has been shown to participate in the attenuation of calcium signaling in CHO and acinar pancreatic cells (18–20). Enough evidence has led to the proposal of RGS4 as a modulator of Ca^{2+} oscillations elicited by many hormones and neurotransmitters, such as ACh (reviewed in Ref. 7). Participation of RGS4 in regulation of epinephrine and norepinephrine secretion in adrenal glands is therefore likely. Consistent with this hypothesis, we show that adrenal glands from $RGS4^{-/-}$ mice secrete larger amounts of epinephrine and norepinephrine than $RGS4^{+/+}$ mice, even in the absence of any stimulation, resulting in increased circulating catecholamines in these $RGS4^{-/-}$ mice.

Catecholamines play a major role in the stimulation of lipolysis in WAT through the β-adrenergic receptors (1). The increased levels of norepinephrine and epinephrine that we observed in serum of $RGS4^{-/-}$ compared with $RGS4^{+/+}$ mice are likely translated into higher basal lipolytic rate in WAT, which in turn results in increased FFA release and accumulation of circulating FFAs. Deregulation of the lipolytic process leading to increased circulating FFA levels, such as observed in $RGS4^{-/-}$ mice, results in increased lipid uptake and lipid accumulation in liver. Liver steatosis in $RGS4^{-/-}$ mice is a consistent finding in our study. When adipose tissue is overloaded with lipids or when lipolysis is abnormally elevated, liver and to some extent muscle can

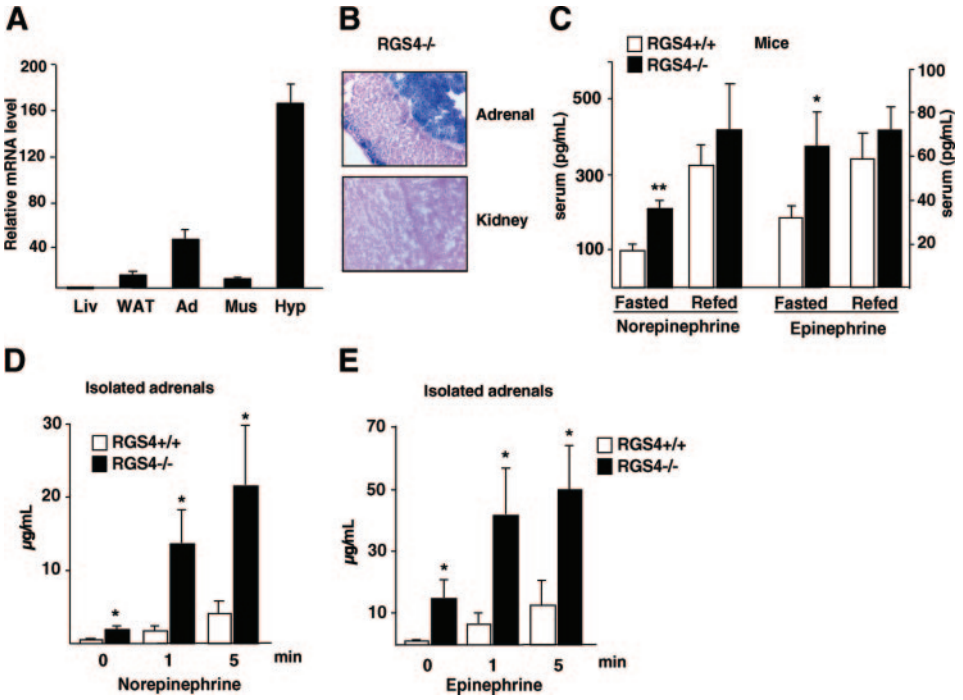

FIG. 5. Increased catecholamine secretion in $RGS4^{-/-}$ mice. A, *RGS4* expression in mouse tissues. Liv, Liver; Ad, adrenals; Mus, muscle; Hyp, hypothalamus. B, Representative β-gal staining of adrenal glands and kidney sections of $RGS4^{-/-}$ mice as indicated. C, Quantification of serum concentration of norepinephrine and epinephrine in overnight-fasted and 4 h-refed 23-wk-old mice ($RGS4^{+/+}$, n = 5, $RGS4^{-/-}$, n = 5). Norepinephrine (D) and epinephrine (E) concentrations were measured at the indicated time points after stimulation of acute adrenal slices (n = 6) with acetylcholine (100 μM).

buffer the increased circulating FFAs, which are toxic for other tissues, specially for pancreatic β-cells. This protective mechanism is, however, transient because further TG accumulation in liver results in both increased glucose synthesis from FFAs and release of TG included in very low-density lipoproteins, which could impair peripheral tissue function, in particular pancreatic β-cell insulin secretion (21). Liver steatosis is associated with hepatic insulin resistance, which means that the liver is less sensitive to the suppressive effects of insulin on hepatic glucose production. If the ability of insulin to suppress the hepatic output of glucose is decreased, then this contributes to postprandial hyperglycemia and hyperlipidemia (22). This is the case for $RGS4^{-/-}$ mice, which show an increased glucose levels and a lower glucose tolerance, compared with $RGS4^{+/+}$ mice. This effect is further increased in mice fed a high-fat diet. Furthermore, quantification of lipid content in another metabolic tissue, such as muscle demonstrated an increase in TG content in $RGS4^{-/-}$ compared with $RGS4^{+/+}$ muscles. Increased lipid content in muscle inhibits insulin action in these cells, which could contribute to the observed insulin resistance in $RGS4^{-/-}$ mice. Glucose intolerance in $RGS4^{-/-}$ mice is therefore the result of the observed increase in circulating FFAs, liver steatosis, and increased muscle lipid content in these mice. Elevated plasma FFAs and liver steatosis are independent predictors of progression to insulin resistance (23). Chronically elevated FFA has several detrimental effects on glucose homeostasis. FFAs may compete with glucose for entry into muscle cells. In addition, excessive fat oxidation inhibits pyruvate dehydrogenase, resulting in the inhibition of glucolysis. These major effects of FFAs are reflected in $RGS4^{-/-}$ mice by increased glucose and insulin levels, and glucose intolerance (Fig. 3).

In summary, we have shown that RGS4, which has been so far described as a regulator of neurological processes, is also implicated in the control of adipose tissue lipolysis through the regulation of catecholamine secretion. As a result, $RGS4^{-/-}$ mice have increased circulating FFAs, liver steatosis, and glucose intolerance. RGS4 could be therefore considered as a new target for the treatment of insulin resistance and type 2 diabetes. Inhibition of RGS protein signaling has been proposed for the treatment of several neurological pathologies, such as depression, epilepsy, or pain (8). Concerning metabolic abnormalities, such as obesity or inhibition of RGS4 with specific inhibitors (24), could result in increased lipolysis and reduced adiposity in the long term. Concomitant treatments to avoid accumulation of lipids in liver and muscle should be, however, also envisaged.

Acknowledgments

Emilie Blanchet, Jacques Teyssier, and Corinne Henriquet are acknowledged for their technical assistance. We thank all the members of Lluis Fajas laboratory for their helpful support and discussion.

Received May 14, 2008. Accepted July 8, 2008.

Address all correspondence and requests for reprints to: Institut National de la Santé et de la Recherche Médicale Unité 834, Centre Régional de Lutte Contre le Cancer Val d'Aurelle, Parc Euromedecine, 34298 Montpellier, France. E-mail: l.fajas@valdorel.fnclcc.fr.

This work was supported by grants from La Ligue Nationale Contre le Cancer, Institut National de la Santé et de la Recherche Médicale, Fondation Pour la Recherche Medicale, Agence Nationale de la Recherche, and Association pour la Recherche sur le Cancer.

Disclosure Statement: The authors have nothing to disclose.

References

1. **Langin D** 2006 Adipose tissue lipolysis as a metabolic pathway to define pharmacological strategies against obesity and the metabolic syndrome. Pharmacol Res 53:482–491
2. **DeHaven J, Sherwin R, Hendler R, Felig P** 1980 Nitrogen and sodium balance and sympathetic-nervous-system activity in obese subjects treated with a low-calorie protein or mixed diet. N Engl J Med 302:477–482
3. **Arner P** 2005 Human fat cell lipolysis: biochemistry, regulation and clinical role. Best Pract Res Clin Endocrinol Metab 19:471–482
4. **Tentolouris N, Liatis S, Katsilambros N** 2006 Sympathetic system activity in obesity and metabolic syndrome. Ann NY Acad Sci 1083:129–152
5. **Zimmermann R, Strauss JG, Haemmerle G, Schoiswohl G, Birner-Gruenberger R, Riederer M, Lass A, Neuberger G, Eisenhaber F, Hermetter A, Zechner R** 2004 Fat mobilization in adipose tissue is promoted by adipose triglyceride lipase. Science 306:1383–1386
6. **Cabrera-Vera TM, Vanhauwe J, Thomas TO, Medkova M, Preininger A, Mazzoni MR, Hamm HE** 2003 Insights into G protein structure, function, and regulation. Endocr Rev 24:765–781
7. **Hollinger S, Hepler JR** 2002 Cellular regulation of RGS proteins: modulators and integrators of G protein signaling. Pharmacol Rev 54:527–559
8. **Neubig RR, Siderovski DP** 2002 Regulators of G-protein signalling as new central nervous system drug targets. Nat Rev Drug Discov 1:187–197
9. **Grillet N, Pattyn A, Contet C, Kieffer BL, Goridis C, Brunet JF** 2005 Generation and characterization of Rgs4 mutant mice. Mol Cell Biol 25:4221–4228
10. **Ishii M, Inanobe A, Fujita S, Makino Y, Hosoya Y, Kurachi Y** 2001 Ca(2+) elevation evoked by membrane depolarization regulates G protein cycle via RGS proteins in the heart. Circ Res 89:1045–1050
11. **Riley B, Kendler KS** 2006 Molecular genetic studies of schizophrenia. Eur J Hum Genet 14:669–680
12. **Hansen JB, Petersen RK, Larsen BM, Bartkova J, Alsner J, Kristiansen K** 1999 Activation of peroxisome proliferator activated receptor G bypasses the function of the retinoblastoma protein in adipocyte differentiation. J Biol Chem 274:2386–2393
13. **Picard F, Gehin M, Annicotte J, Rocchi S, Champy MF, O'Malley BW, Chambon P, Auwerx J** 2002 SRC-1 and TIF2 control energy balance between white and brown adipose tissue. Cell 11:931–941
14. **Moser T, Neher E** 1997 Rapid exocytosis in single chromaffin cells recorded from mouse adrenal slices. J Neurosci 17:2314–2323
15. **Fajas L, Annicotte JS, Miard S, Sarruf D, Watanabe M, Auwerx J** 2004 Impaired pancreatic growth, β cell mass, and β cell function in E2F1($^{-/-}$) mice. J Clin Invest 113:1288–1295
16. **Douglas WW, Rubin RP** 1961 Mechanism of nicotinic action at the adrenal medulla: calcium as a link in stimulus-secretion coupling. Nature 192:1087–1089
17. **Douglas WW, Rubin RP** 1961 The role of calcium in the secretory response of the adrenal medulla to acetylcholine. J Physiol 159:40–57
18. **Ho G, Wang Y, Jones PG, Young KH** 2007 Activation of serum response element by D2 dopamine receptor is governed by Gβγ-mediated MAPK and Rho pathways and regulated by RGS proteins. Pharmacology 79:114–121
19. **Xu X, Zeng W, Popov S, Berman DM, Davignon I, Yu K, Yowe D, Offermanns S, Muallem S, Wilkie TM** 1999 RGS proteins determine signaling specificity of Gq-coupled receptors. J Biol Chem 274:3549–3556
20. **Riddle EL, Schwartzman RA, Bond M, Insel PA** 2005 Multi-tasking RGS proteins in the heart: the next therapeutic target? Circ Res 96:401–411
21. **Lewis GF, Carpentier A, Adeli K, Giacca A** 2002 Disordered fat storage and mobilization in the pathogenesis of insulin resistance and type 2 diabetes. Endocr Rev 23:201–229
22. **den Boer MA, Voshol PJ, Kuipers F, Romijn JA, Havekes LM** 2006 Hepatic glucose production is more sensitive to insulin-mediated inhibition than hepatic VLDL-triglyceride production. Am J Physiol Endocrinol Metab 291: E1360–E1364
23. **Tataranni PA, Baier LJ, Paolisso G, Howard BV, Ravussin E** 1996 Role of lipids in development of noninsulin-dependent diabetes mellitus: lessons learned from Pima Indians. Lipids 31(Suppl):S267–S270
24. **Roman DL, Talbot JN, Roof RA, Sunahara RK, Traynor JR, Neubig RR** 2007 Identification of small-molecule inhibitors of RGS4 using a high-throughput flow cytometry protein interaction assay. Mol Pharmacol 71:169–175